Theor Chem Acc (2011) 130:955–963
DOI 10.1007/s00214-011-1057-y

REGULAR ARTICLE

Computational study on the partial dechlorination of the pesticide chloropicrin by sulfur species

Oscar N. Ventura · Patricia Saenz-Méndez · Fiorentina Bottinelli

Received: 31 May 2011 / Accepted: 22 September 2011 / Published online: 3 November 2011

Abstract Density functional and MP2 calculations with extended basis sets were performed on the species participating in both the previously suggested and a newly proposed mechanisms of partial dechlorination of chloropicrin by simple sulfur species, both in gas phase and in a simulated water environment. Thermochemistry of both mechanisms in the gas phase was also studied using the chemical models G3 and G4. It is shown that the previously proposed reductive dehalogenation is not thermodynamically feasible at room temperature, as it should be according to the experimental evidence. Although inclusion of the solvent improves the results with respect to gas phase, the thermodynamics of the proposed mechanism by Zheng et al. is still unfavorable for obtaining the experimental products. An alternative mechanism is then proposed, involving the formation of HSCl, which is the intermediate that then undergoes redox reactions. Such a mechanism is exothermic and spontaneous, according to the computational results, and produces elementary sulfur in agreement with the experimental facts.

Dedicated to Professor Akira Imamura on the occasion of his 77th birthday and published as part of the Imamura Festschrift Issue.

Electronic supplementary material The online version of this article (doi:10.1007/s00214-011-1057-y) contains supplementary material, which is available to authorized users.

O. N. Ventura (✉) · P. Saenz-Méndez · F. Bottinelli
Computational Chemistry and Biology Group, DETEMA,
Facultad de Química, UdelaR, CC1157,
11800 Montevideo, Uruguay
e-mail: onv@fq.edu.uy

P. Saenz-Méndez
Physical Organic Chemistry and Bioprocesses Group,
DQO, Facultad de Química, UdelaR, CC1157,
Avda. Gral. Flores 2124, 11800 Montevideo, Uruguay

Keywords Hydrogen sulfide species · Chloropicrin · Dechlorination · Density functional theory

1 Introduction

Organochlorine chemicals present in the environment are not only of anthropogenic origin. There are over 3,000 naturally occurring species containing chlorine, in addition to those produced by human activities [1]. For instance, it was discovered that even vinyl chloride, previously thought to be a true xenobiotic, is produced and released naturally into the environment [2]. As a consequence, certain microorganisms have evolved and developed the ability to dehalogenate different classes of organochlorine species, including xenobiotics. These microorganisms have dehalogenating enzymes acting through reductive dehalogenation [3, 4] (anaerobic bacteria), oxidative [5, 6], or dehydrohalogenation mechanisms, among others [7].

Environmentally, the existence of a large number of industries which effluents contain organochlorine chemicals makes the study of their transformation into harmless compounds, or even their complete mineralization, an important subject. For this reason, we undertook basic computational studies of the many reactions involved in these processes of detoxification of simple and widespread organochlorine compounds.

Chloropicrin (trichloronitromethane or nitrochloroform) is a pesticide used as a soil fumigant due to its broad biocidal properties, mainly in high-value crops such as strawberries, raspberries, peppers, onions, snuff, flowers, and many others. Even though it is not an air pollutant [8], its chemical interactions in the ground and the possibility of transport to other surface layers are of great concern. Additionally, it has been shown that chloropicrin is also

produced in the disinfection of nitrite-containing water, when it is treated with chlorine or chlorine dioxide after ozonation [9]. Under the effect of solar radiation, chloropicrin undergoes slow photochemical decomposition. Residual nitrites and nitrosamines in the environment may appear because of that reason.

It is well known that bacteria such as *Pseudomonas putida* can dehalogenate chloropicrin [10]. The metabolic mechanism involves the reaction with GSH (reduced glutathione) and the intervention of some enzymes (such as cytochrome P450 monooxygenases), leading to nitromethane as the final product. Sparks et al. [11] studied in detail this mechanism using HPLC to track products from the reaction of chloropicrin with [glycine-2-3H] GSH. They noted the rapid initial formation of dichloronitromethane that is subsequently transformed to chloronitromethane (and presumably to nitromethane later). Zheng et al. studied experimentally the dechlorination mechanism of chloropicrin and 1,3-dichloropropene by hydrogen sulfide species using HS^- [12]. They determined that the dechlorination of 1,3-dichloropropene takes place through a S_N2 nucleophilic substitution, but that dechlorination of chloropicrin involves a redox mechanism, where sulfur passes from S^{-2} to S^0 while chloride anion is released. They found that chloropicrin reacts quickly when mixed with HS^-, producing a black precipitate of elementary sulfur. Dichloronitromethane concentration increases subsequently and begins later to decrease while the concentration of chloronitromethane increases. The final step produces the nonhalogenated compound nitromethane.

In this study, we explored the reaction pathways for reductive dehalogenation of chloropicrin based initially on the mechanism proposed by Zheng et al. [12]. Due to the results obtained, we propose a modified mechanism involving abstraction of a chlorine atom to form HSCl as an intermediate, which later participates in the oxidation–reduction step. Finally, we determined thermochemical data for all these species using density functional, post-Hartree–Fock, and model chemistry methods.

2 Theoretical methods

Full geometry optimizations of chloropicrin, reaction intermediates, and transition states were performed at the density functional level, using the B3LYP [13] and PBE0 [14] methods. Both are adiabatically connected methods, implementing different exchange and correlation potentials. Second-order Møller-Plesset (MP2) theory was used [15] for the same goal. Increasingly larger 6-31+G(d,p), 6-311++G(2df,2pd), and 6-311++G(3d2f,2pd) Pople basis sets were used in both DFT and MP2 calculations. Analytical second derivatives were calculated in all cases, both to verify the character of the stationary points found and for obtaining zero-point vibrational energies and corrections to enthalpies and free energies, as well as IR spectra within the harmonic approximation. Enthalpies of reaction and formation were determined using the above-mentioned DFT and MP2 methods, as well as the G3 and G4 model chemistry methods [16, 17] (these are composite techniques in which a sequence of well-defined ab initio molecular orbital calculations is performed to arrive at a total energy of a given molecular species). All these calculations were performed in gas phase. In light of the performance observed for the different methods, we chose the PBE0/6-311++G(3d2f,2pd) to examine the proposed and alternative mechanisms in an aqueous environment. The PCM method of Tomasi et al. [18] was employed for these calculations.

The study was started using the experimental information and the redox reaction mechanism proposed by Zheng et al. [12], which will be called Mechanism I.

2.1 Mechanism I

$$Cl_3CNO_2 + HS^-(H_2S) \rightarrow Cl_2CHNO_2 + S + Cl^-(HCl) \quad (1)$$

$$Cl_3CNO_2 + 2HS^-(H_2S) \rightarrow ClCH_2NO_2 + 2S + 2Cl^-(2HCl) \quad (2)$$

$$Cl_2CHNO_2 + HS^-(H_2S) \rightarrow ClCH_2NO_2 + S + Cl^-(HCl) \quad (3)$$

$$ClCH_2NO_2 + HS^-(H_2S) \rightarrow CH_3NO_2 + S + Cl^-(HCl) \quad (4)$$

On the basis of our initial results for Mechanism I, we also explored the possibility of an alternative mechanism for reaction (1), in which the HS^- anion removes a chlorine atom from chloropicrin following these three steps.

2.2 Mechanism II

$$Cl_3CNO_2 + HS^- \rightarrow Cl_2CNO_2^- + HSCl \quad (5)$$

$$HSCl + HS^- \rightarrow HCl + HS_2^- \quad (6)$$

$$Cl_3CNO_2 + HS_2^- \rightarrow Cl_2CNO_2^- + HCl + S_2 \quad (7)$$

and similar reactions up to complete dechlorination. These reactions should proceed in the following way

$$Cl_2CNO_2^- + HCl \rightarrow Cl_2CHNO_2 + Cl^- \quad (8)$$

$$Cl_2CHNO_2 + HS^- \rightarrow ClCHNO_2^- + HSCl \quad (9)$$

$$Cl_2CHNO_2 + HS_2^- \rightarrow ClCHNO_2^- + HCl + S_2 \quad (10)$$

$$ClCHNO_2^- + HCl \rightarrow ClCH2NO_2 + Cl^- \quad (11)$$

$$ClCH_2NO_2 + HS^- \rightarrow CH_2NO_2^- + HSCl \quad (12)$$

$$ClCH_2NO_2 + HS_2^- \rightarrow CH_2NO_2^- + HCl + S_2 \quad (13)$$

$$CH_2NO_2^- + HCl \rightarrow CH_3NO_2 + Cl^- \quad (14)$$

It must be observed also that reaction (6) is not unique and can occur recursively, in the following way

$$HSCl + HS_n^- \rightarrow HCl + HS_{n+1}^- \quad (15)$$

limited only by the stability of the polysulfide and the reaction of formation of solid sulfur

$$HSCl + HS_n^- \rightarrow H_2S + Cl^- + S_n \quad (16)$$

Polysulfides formed in reactions (15) can interact with any of the derivatives of chloropicrin, in the following general way

$$Cl_pCH_{3-p}NO_2 + HS_n^- \rightarrow Cl_{p-1}CH_{3-p}NO_2^- + HCl + S_n \quad (17)$$

We will focus in this paper only on the discussion of reactions (5–7), to establish the feasibility of this alternative mechanism, leaving further studies for the future. The results obtained for both mechanisms are reported in the following. All calculations were performed using the G03 set of computer codes [19].

3 Results

The most significant optimized geometrical parameters of chloropicrin calculated at each theoretical level as well as the experimental structure determined by electron diffraction [20] are shown in Table 1. PBE0 is known to provide the smallest deviation from the experimental geometries at standard T and P, as confirmed in this case. The quality of B3LYP and MP2 results reported in Table 1 is quite similar, apart from the nitro group for which MP2 results are the worst, probably because of lack of inclusion of enough correlation energy. Inclusion of the solvent field does not significantly affect the calculated geometry.

We compared also the calculated infrared frequencies with the values determined experimentally in the work of Wade et al. [21] and in the work of Haszeldine et al. [22] (see data in Table 2). A reasonable qualitative agreement between theoretical and experimental spectra is noted with respect to the position of the bands, for which the two experimental sets of data are in agreement. However, the three methods report shifts toward larger frequencies in the case of both stretching bands of the nitro group. Using only the results obtained with the larger basis set, the shifts are 55–60 (B3LYP), 110–140 (PBE0), and 10–200 (MP2) cm^{-1}. We consider that the surprisingly good agreement for the MP2 calculation of the symmetric NO_2 stretching is just a coincidence. In our opinion, the shifts reflect the interaction of the strongly polarized nitro group either with the solvent [22] or with the solid matrices [21].

Both DFT methods correctly predict that the band corresponding to the NO_2 asymmetric stretch (without participation of the CCl_3 group) is the most intense. This feature is not described well by the MP2 calculations. The experimental determination disagrees as to the intensity of the symmetric stretching band, weak in the more recent results of Wade et al. [21] and very strong according to Haszeldine [22]. The three methods predict that the symmetric stretch is not weak, but from medium to strong, although MP2 underestimate both NO_2 stretching bands' intensities. Both DFT methods also predict correctly the triplet bands around 900 cm^{-1} with slight shifts according to the theoretical method and the experimental results with respect to which one is comparing.

The interactions with the environment are not considered in our calculations, performed for the molecule in the

Table 1 Experimental and theoretical bond lengths (in Å) and angles (in degrees) for chloropicrin

Parameter[a]	Exp [20]	6-31+G(d,p)			6-311++G(2df,2pd)			6-311++G(3d2f,2pd)[b]		
		B3LYP	PBE0	MP2	B3LYP	PBE0	MP2	B3LYP	PBE0	MP2
d(C–N)	1.594	1.618	1.595	1.581	1.617	1.592	1.576	1.617	1.593 *(1.591)*	1.574
d(N–Oec)	1.190	1.214	1.205	1.233	1.204	1.196	1.217	1.203	1.195 *(1.196)*	1.216
d(N–O al)		1.215	1.207	1.233	1.206	1.198	1.217	1.205	1.197 *(1.199)*	1.216
d(C–Clec)	1.726	1.759	1.743	1.742	1.750	1.734	1.737	1.747	1.731 *(1.731)*	1.732
d(C–Cl al)		1.775	1.757	1.755	1.766	1.749	1.752	1.763	1.746 *(1.746)*	1.746
<CNO ec	113.2	117.3	117.2	117.9	117.1	117.1	117.4	117.1	117.1 *(117.5)*	117.5
<CNO al		114.5	114.4	114.3	114.5	114.4	114.2	114.5	114.3 *(114.6)*	114.2
<NCClec	106.0	109.3	109.2	109.3	109.5	109.6	109.7	109.5	109.6 *(109.5)*	109.6
<NCCl al		106.1	106.1	106.0	106.1	106.1	106.1	106.1	106.1 *(106.1)*	106.1

[a] ec and al stand for eclipsed and alternated with respect to the CCl or NO bonds; [b] values in italics calculated using the PCM method for a dielectric simulating water

Table 2 Experimental and theoretical frequencies (in cm^{-1}) and intensities (in parenthesis, in Km mol) for the transitions in the IR spectrum

Parameter[a]	Exp[b]		6-31+G(d,p)			6-311++G(2df,2pd)[c]		
	[21]	[22]	B3LYP	PBE0	MP2	B3LYP	PBE0	MP2
NO_2str–a	1,615 (vs)	1,610 (vs)	1,698 (252)	1,779 (269)	1,831 (64)	1,675 (276)	1,753 (281)	1,813 (92)
							1,716 (567)	
NO_2str–s	1,310 (w)	1,307 (vs)	1,374 (134)	1,431 (131)	1,319 (71)	1,365 (139)	1,421 (133)	1,321 (82)
							1,423 (203)	
C–N	850 (w)	842 (m)	830 (42)	862 (33)	845 (12)	841 (49)	873 (39)	860 (22)
							876 (51)	
CCl_3 a	910 (m)	895 (s)	871 (178)	917 (177)	937 (146)	865 (166)	913 (163)	919 (143)
							899 (305)	
CNO_2oop–a	880 (s)	858 (s)	842 (140)	883 (149)	894 (161)	841 (115)	882 (124)	880 (140)
							872 (201)	
CCl_3 (oop)	710 (w)		690 (34)	731 (41)	735 (48)	686 (26)	732 (35)	740 (39)
							726 (73)	
CNO_2oop–s	680 (w)		666 (68)	698 (55)	679 (23)	673 (75)	707 (60)	691 (32)
							700 (115)	

[a] *Str* stretching, *oop* out of plane deformation, *s* symmetric, *a* asymmetric; [b] *vs* very strong, *w* weak, *m* medium, *s* shoulder; [c] values in italics calculated using the PCM method for a dielectric simulating water

gas phase. We consider that the differences between the calculated and experimental frequencies for the symmetric and asymmetric stretching bands of the nitro group are due to those interactions. However, there is also a discrepancy between the experimental results themselves. Wade's cryogenic matrices' results indicate that the symmetric band is weak, while Haszeldine results in solution point to a very strong band. IR and UV spectra of several nitroalkanes, other than chloropicrin, were determined also in Haszeldine's work [22]. The intensities of both symmetric and asymmetric stretching bands are very strong (*vs*) in all cases, a fact in disagreement with the results obtained by Wade [21] for chloropicrin. Thus, we conclude that this is an effect of the cryogenic matrix, although we are not able to explain why it does affect only the intensity of the symmetric stretching. However, the results calculated including the solvent field show also that the nitro group asymmetric stretching is the most sensitive to the environment, lending support to the previous considerations.

For all but NO_2 stretching modes, MP2, B3LYP, and PBE0 methods provide results of similar quality. For NO_2, the B3LYP results are closer to the experimental ones. Looking at the geometries, PBE0 is the method providing the best results, while B3LYP gives larger bond lengths. This overestimation of bond lengths by B3LYP makes the oscillator weaker and the corresponding frequency lower. It is similar to experiment, where the bond is weakened by interactions with the environment. Thus, the better agreement of B3LYP in this case is only a fortuitous compensation of errors.

Free energies and enthalpies of reaction at room temperature are shown in Table 3. We have assumed that the G4 model chemistry results are the most accurate, describing in the best possible way the values of relative enthalpies and free energies in the gas phase. Therefore, we included in Table 3 an r.m.s. error for free energies of reaction on one side and enthalpies of reaction on the other, both with respect to the G4 results. The PBE0 method performs much better than either B3LYP or MP2 with the small basis set, but the results are very far from the G4 ones. With the larger basis sets, however, both PBE0 and MP2 values differ from G4 only by a few kJ/mol. The results obtained with the richest basis set are comparable to those obtained at the G3 level. B3LYP on the contrary underestimates the enthalpies and free energies of reaction by tenths of kJ/mol for all reactions except (4a).

All reactions are highly endothermic, and the free energies are positive. It is true that precipitation of solid sulfur would displace the equilibrium toward the right-hand side and that inclusion of solvation effects lowers the energy differences, but the whole picture seems to disagree with the experimental evidence of the reactions occurring easily at room temperature. From these results, we can conclude that dechlorination of chloropicrin would not occur according to Mechanism I.

Therefore, based on experimental data reported by Zheng et al. [12], we studied the alternative Mechanism II in which HS^- removes a chlorine atom from chloropicrin according to reaction (5) giving HSCl (this isomer was preferred because in a theoretical study at different levels

Table 3 Relative free energies (first entry) and enthalpies (second entry) for reactions in Mechanism I (1–4) and (1a–4a) (in kJ mol^{-1})

	6-31+G(d,p)			6-311++G(2df,2pd)			6-311++G(3d2f,2pd)[a]			G3	G4
	B3LYP	PBE0	MP2	B3LYP	PBE0	MP2	B3LYP	PBE0	MP2		
(1)	44.1	63.8	44.8	63.4	86.3	90.3	70.2	93.3 (68.4)	97.2	98.1	92.1
	72.6	93.9	74.6	93.6	117.7	121.3	99.8	124.1 (103.8)	128.0	127.9	122.4
(2)	103.5	141.8	100.8	143.4	188.3	192.4	155.1	199.9 (156.1)	202.9	204.7	197.8
	161.0	200.3	162.6	201.8	247.1	252.9	213.2	258.7 (216.3)	263.7	264.3	255.7
(3)	59.4	78.0	56.0	80.0	102.0	102.1	84.9	106.6 (87.7)	106.4	106.6	105.6
	88.3	106.4	88.0	108.2	129.4	131.6	113.4	134.6 (112.5)	137.0	136.5	133.3
(4)	63.0	81.9	53.4	80.8	102.7	99.0	86.3	107.9 (95.4)	103.9	101.8	99.4
	94.4	113.6	82.3	113.4	135.4	129.0	117.7	139.6 (120.3)	133.7	133.2	130.8
(1a)	124.5	142.0	124.7	138.1	158.1	161.7	144.3	164.4 (151.9)	168.1	165.3	163.0
	157.2	176.2	158.8	172.5	193.7	196.9	178.2	199.5 (191.4)	202.2	199.3	197.5
(2a)	264.6	298.6	261.1	293.1	332.4	335.8	303.8	342.8 (323.5)	345.7	339.6	340.1
	330.7	365.6	331.5	360.1	399.8	404.7	370.5	410.1 (392.2)	415.1	407.8	406.7
(3a)	139.7	156.1	136.0	154.6	173.8	177.8	159.0	177.8 (171.1)	181.5	173.7	176.6
	172.9	188.8	172.2	187.1	205.4	207.2	191.7	210.0 (200.1)	211.9	207.9	208.5
(4a)	143.4	160.0	133.4	155.5	174.5	170.4	160.4	179.1 (178.8)	175.0	168.9	170.3
	179.0	196.0	166.5	192.3	211.4	204.6	196.1	215.0 (208.0)	207.0	204.6	206.0
rmse	22.2	12.4	22.8	12.9	2.2	0.7	10.0	2.0	2.1	1.6	
	22.1	12.5	23.4	13.0	2.3	1.2	10.1	1.8	1.9	1.5	

First four rows refer to the reactions obtained using HS^-, and the second four rows correspond to reactions using H_2S as a reactant

[a] Numbers in parenthesis are the enthalpies obtained in water, using PCM for the simulation

of calculation it was determined that HSCl is much more stable than its isomer HClS [24]).

HSCl is not an easy target. Agarwal et al. [23] in 1985 studied the complex between H_2S and different halogens using vibrational spectroscopy in cryogenic matrices. Signals registered at 485 cm^{-1} in Ar and 470 cm^{-1} in N_2 were tentatively assigned to the HSCl species. They could not isolate this species and proposed that HSCl is probably an intermediate in the production of polysulfide species, according to the following equation:

$$HSCl + H_2S_{(n-1)} \rightarrow HCl + H_2S_n \quad (18)$$

The final step would be the precipitation of elementary sulfur as S8. Using this precedent, we propose that the HSCl species formed in reaction (5) would further react with HS^- to give (dissociated) HCl and the anionic polysulfide species HS_2^- which in turn would react with an additional chloropicrin molecule to give the dichloronitromethane anion and elementary sulfur as S_2 (reactions 6 and 7). In fact, other polysulfide species could be formed according to reaction (17), but we will focus on the simpler example in this paper.

Structural and vibrational information of HSCl determined in this work is shown in Table 4 and compared also Resende and Ornellas' previous results [25]. Structural parameters do not show a great variation with the different methods of calculation and/or basis set. Uncorrected vibrational frequencies display larger differences even though the trend remains invariant. The experimental frequency assigned to the HSCl species by Agarwal et al. [23]—shoulder at 485 cm^{-1} in Ar and 470 cm^{-1} in N_2 cryogenic matrices—corresponds reasonably well to the lowest frequency calculated in this work, 544 and 548 cm^{-1} with the MP2 and PBE0 methods, and the largest basis set. This band corresponds to the ClS stretching mode, as assigned experimentally, and has an intensity ratio of 13:1 with respect to the HSCl angle band and HS stretching bands, in the range 920–930 and 2,700–2,770 cm^{-1}, respectively.

Table 5 shows calculated enthalpy and free energy of reaction for reactions (5–7) obtained at different levels of theory. Reactions, where all the reactant and product anions are protonated to convert them in neutral species, are also included and labeled as (5a–7a) for comparison with the data in Table 3.

It is clear that reaction (5) is spontaneous and exothermic according to all the calculations, which is now in agreement with the experimental data showing spontaneous reaction at room temperature. It is also evident that the drive comes from the attack of the sulfide [or, latter, polysulfide as in equation (7)] and the larger stabilization of the charge on the $Cl_3CNO_2^-$ anion with respect to the HS^- anion. Although these are the general trends for reaction (5), the theoretical methods do not afford a well-converged result

Table 4 Theoretical bond lengths (in Å), angles (in deg), and vibrational frequencies (in cm^{-1}) for HSCl

Method		Basis set	d(S–Cl)	d(S–H)	<HSCl	SCl str	HSCl bnd	HS str
DFT	B3LYP	6-31+G(d,p)	2.082	1.351	96.0	497	906	2,671
		6-311++G(2df,2pd)	2.059	1.345	95.9	515	909	2,668
		6-311++G(3d2f,2pd)	2.054	1.345	95.9	512	911	2,666
	PBE0	6-31+G(d,p)	2.050	1.347	96.2	531	926	2,721
		6-311++G(2df,2pd)	2.029	1.344	95.9	552	921	2,704
		6-311++G(3d2f,2pd)	2.025	1.344	96.0	548	923	2,702
MP2		6-31G(d,p) [25]	2.047	1.333	96.1	542	964	2,819
		6-31+G(d,p)	2.051	1.333	95.9	536	960	2,818
		6-31G(2df,2pd) [25]	2.033	1.333	95.7	565	940	2,766
		cc-pVTZ [25]	2.038	1.338	95.5	555	928	2,752
		6-311++G(2df,2pd)	2.036	1.334	95.5	557	933	2,767
		6-311++G(3d2f,2pd)	2.033	1.334	65.6	544	933	2,766
CCSD(T)		6-31G(d,p) [25]	2.066	1.338	95.9	510	944	2,753
		6-31G(2df,2pd) [25]	2.051	1.304	95.5	539	922	2,714
		cc-pVTZ [25]	2.056	1.349	95.3	529	911	2,696

Table 5 Relative free energies (first row of each entry) and enthalpies (second row) for the reactions in Mechanism II, (5–7) (in kJ mol^{-1})

	6-31+G(d,p)			6-311++G(2df,2pd)			6-311++G(3d2f,2pd)			G3	G4
	B3LYP	PBE0	MP2	B3LYP	PBE0	MP2	B3LYP	PBE0	MP2		
(5)	−61.9	−52.6	−12.6	−78.3	−71.4	−33.1	−74.5	−67.0 *(−14.6)*	−39.0	−34.7	−42.2
	−54.9	−44.1	−4.4	−69.5	−61.2	−24.7	−66.2	−57.1 *(−5.5)*	−30.7	−25.1	−34.8
(6)	−79.3	−85.6	−86.8	−76.4	−82.1	−87.6	−77.1	−82.8 *(−55.5)*	−88.4	−83.2	−84.3
	−79.1	−85.5	−86.7	−76.2	−81.9	−87.5	−76.9	−82.7 *(−55.4)*	−88.2	−82.9	−84.1
(7)	−88.1	−66.0	−58.8	−90.5	−67.5	−35.8	−86.4	−63.0 *(−39.4)*	−33.2	−31.7	−30.7
	−51.9	−28.0	−20.9	−52.3	−27.6	2.4	−48.7	−23.4 *(−0.6)*	5.0	7.3	6.1
(5a)	−7.3	1.8	28.5	−17.3	−10.1	11.7	−12.9	−5.4 *(−14.0)*	7.5	8.8	1.8
	−3.3	7.2	33.6	−11.7	3.5	18.0	−7.9	0.6 *(−3.4)*	11.3	13.8	7.5
(6a)	−42.4	−47.8	−50.0	−41.5	−46.4	−49.6	−41.4	−46.3 *(−46.9)*	−46.8	−43.0	−44.7
	−46.0	−51.5	−53.7	−45.1	−50.1	−53.2	−45.0	−50.0 *(−50.5)*	−52.2	−48.3	−48.3
(7a)	−70.4	−49.4	−54.5	−64.4	−41.9	−29.0	−60.6	−37.9 (−47.5)	−25.1	−28.4	−26.3
	−33.3	−10.7	−15.9	−25.6	−1.8	10.8	−22.3	1.6 (−3.5)	13.2	11.5	12.6

Neutral reactions, where all the anions were protonated, are labeled (5a–7a) for comparison with the results included in Table 3. Italized numbers are the results obtained using the PCM method at the PBE0/6-311++G(3d2f,2pd) level of calculation

for the enthalpies or free energies of reaction, contrary to what happened in the case of reaction (1). The more sophisticated available results for these reactions are the G4 and MP2 calculations, which are reasonably in agreement with each other. This is fortuitous, since the Gaussian-4 (G4) chemical model includes correlation energy up to the CCSD(T) level. Differences with respect to the G3 method include a larger polarization space for second-row atoms and a better calculation of the correlation energy. G3 and G4 results are generally coincident, but it has been shown that differences larger than 10 kJ/mol can exist for the gas phase enthalpy of formation of heavily substituted halocarbons [26]. Both DFT methods fail to reproduce the G4 results for this reaction. Two reasons can be thought as the origin of this discrepancy, the different level of precision in the description of the C–Cl and S–Cl bonds in both sides of the equation and of the charge distribution on HS^- as compared to $CCl_2NO_2^-$. This latter aspect can be checked protonating the anions on both sides of the reaction, obtaining then the nonionic reaction of chloropicrin with hydrogen sulfide to give dichloronitromethane plus ClSH, reaction labeled as (5a) in Table 5. Although there is still a difference, now the PBE0 method behaves as well (or as bad) as MP2 or G3 with respect to G4.

In order to study reaction (5) in more detail, the ion-molecular complex consisting of chloropicrin and HS^- was

optimized. We found that the S–H distance in this complex is very similar to that found in the optimized structure of HSCl, whereas the S–Cl distance is about 0.25 Å longer. The formation of this complex is energetically favorable in gas phase, mainly due to the larger size of the anion, which allows delocalization of the negative charge. The enthalpy difference between the complex and the isolated fragments in the gas phase is −100 kJ/mol for B3LYP and −95.8 kJ/mol for PBE0 (using the 6-311++G(2df,2pd) basis set). Therefore, the complex is highly stable with respect to the chloropicrin and the HS^- anion, and its enthalpy is above that of the HSCl molecule and the chloropicrin anion infinitely separated.

Figure 1 shows the transition structure connecting the ion-molecular complex with the molecule of HSCl and the chloropicrin anion at the PBE0/6-311++G(2df,2pd) level. It has to be noted that there is almost no C–Cl bond, the S–Cl distance corresponding almost exactly to that found in HSCl, while the $CCl_2NO_2^-$ anion is nearly planar. The transition state at this level is 20 kJ/mol higher in energy than the initial complex, but since this one is very stable with respect to the reactants, the transition state is in fact 20 kJ/mol below the infinitely separated chloropicrin and HS^- anion. On the other side, the transition state is 61 kJ/mol above the products, which clearly implies an exothermic reaction as we concluded previously from the thermodynamic results.

Considering what we have discussed before, the alternative mechanism proposed (Mechanism II) would consist of reactions (9) and (19–22),

$$Cl_3CNO_2 + HS^- \rightarrow Cl_2CNO_2^- + HSCl \quad (5)$$

$$HSCl + HS_n^- \rightarrow H^+ + Cl^- + HS_{n+1}^- \quad (n = 1, 2, \ldots) \quad (19)$$

$$CCl_2NO_2^- + H^+ \rightarrow CHCl_2NO_2 \quad (20)$$

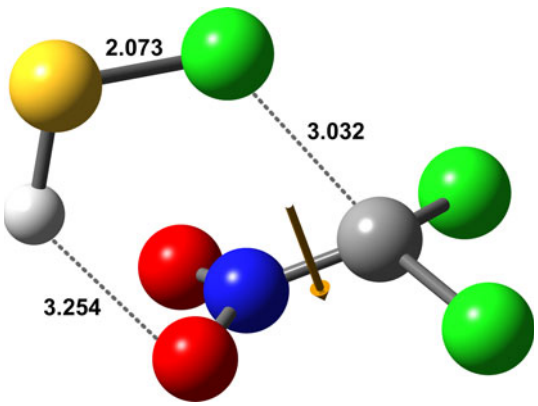

Fig. 1 Structure of the transition state connecting the ion-molecular complex with the molecule of HSCl and the chloropicrin anion. The main distances obtained at the PBE0/6-311++G(2df,2pd) level are shown in the figure. The *arrow* shows the direction and magnitude of the transition vector

$$CHCl_2NO_2 + HS^- \rightarrow CHClNO_2^- + HSCl \quad (21)$$

$$CH_{3-p}Cl_pNO_2 + HS_n^- \rightarrow CH_{3-p}Cl_{p-1}NO_2^- + H^+ + Cl^- + S_n \quad (p = 1, 2, 3) \quad (22)$$

We have already demonstrated that reaction (5) is exothermic and spontaneous, with a small barrier for the formation of HSCl. Reactions (19) lead to the formation of polysulfides and are discussed below. The presence of protons in the media, following the formation of polysulfides, leads to the neutralization reaction (20). The pattern of reaction (5) is reproduced for dichloronitromethane and chloronitromethane as shown in reaction (21). Finally, precipitation of sulfur would occur as per reactions (22), which become competitive when n is larger than 1. Regarding reaction (19), we studied in this work the simplest case, $n = 1$, which is reaction (6)

$$HSCl + HS^- \rightarrow HCl + HS_2^- \quad (6)$$

This reaction is also spontaneous and exothermic at all levels of calculation (see Table 5), which are now in very good agreement among themselves. Thus, this is a feasible way of decomposition of HSCl. Notice that all the methods give very similar enthalpy and free energy values for this reaction, even using the small basis set. This was not the case for reaction (5), and we will see that it is not either for reaction (7).The last step in the mechanism would be reaction (22). We will again consider only the simplest case, $n = 1$, which is reaction (7)

$$CCl_3NO_2 + HS_2^- \rightarrow CCl_2NO_2^- + HCl + S_2 \quad (7)$$

As shown in Table 5, all methods predict the reaction to be spontaneous. As in the case of reaction (5), both DFT methods predict a much larger free energy and enthalpy than the ab initio methods, which in this case predict that the reactions are slightly endothermic. The whole process is, however, exothermic at all levels of calculation, although they are not quantitatively in agreement among themselves. We think then that Mechanism II occurring through the HSCl intermediate formed by chlorine abstraction from chloropicrin explains the experimental data and should be preferred over Mechanism I.

4 Conclusions

Optimum structures for chloropicrin, HSCl, and related species have been obtained at the DFT and post-Hartree–Fock levels using sufficiently large basis sets. The structure of the transition state that connects the ion-molecular complex between HS^- and chloropicrin with the molecules of HSCl, and the chloropicrin anion was also calculated in gas phase.

Examining the detailed alternative mechanism of dechlorination of chloropicrin by sulfur species presented in this work, we could suggest that while the overall reaction is an oxidation–reduction step, the active species is not chloropicrin itself, but the intermediate HSCl species formed by the abstraction of Cl from chloropicrin.

The main suggestion of this study is that the mechanism of dechlorination is mediated by HSCl. The suggested intermediate can explain the appearance of polysulfides. They react in turn with chloropicrin and the dechlorinated products generating the sulfur precipitate. A simplified way to write the mechanism included in Eqs. 5–7 would be as

$$CCl_3NO_2 + HS^- \rightarrow CCl_2NO_2^- + HCl + S \qquad (13)$$

However, while this reaction is spontaneous and exothermic, as supported by the experimental data, it hides the crucial role of HSCl and polysulfide species.

Note added in proof It has been shown that a more complete consideration of the conformation of biomolecules in aqueous solution and their corresponding vibrational spectra are in many cases improved by taking into account specific interactions between the solute and solvent molecules [27]. Hence, to model chloropicrin in aqueous solution, we have included the effect of specific interactions with discrete solvent molecules in our highest level model. The rotational potential of the nitro group at the PBE0/6-311++G(3d2f,2pd) level shows that the more stable conformers both in the gas phase and including the continuum are those where one NO bond eclipses one CCl bond. The rotational barrier is however extremely low, <0.5 kJ mol^{-1}, implying an almost free rotation. Therefore, it cannot be excluded that specific interactions with solvent molecules would stabilize some other conformer or conformers.

A more complete description of the solvent was then produced in the following way. A molecular dynamics calculation at the semi-empirical PM3 level was run, immersing the chloropicrin molecule in a cubic box of water molecules, each side being 18 Å long. After equilibration at room temperature, the 28 water molecules nearest to the chloropicrin solute were chosen and the whole system submitted to full geometry optimization at the PBE0/6-31+G(d,p) level. A true minimum was obtained with all positive eigenvalues of the Hessian. The main geometrical parameters of the gas phase and solvated structures are shown in Table 6, according to the labeling shown in Fig. 2.

Table 6 Geometrical parameters of chloropicrin calculated at the PBE0/6-31+G(d,p) level in gas phase, within the continuum simulation of the aqueous solvent and in the cluster of 28 water molecules

Parameter	Gas phase	Continuum	Cluster
R(N2O4)	1.196	1.205	1.202
R(N2O3)	1.198	1.208	1.213
R(C1N2)	1.592	1.594	1.585
R(C1Cl5)	1.734	1.741	1.745
R(C1Cl6)	1.749	1.756	1.772
R(C1Cl7)	1.749	1.756	1.733
Θ(O3N2O4)	128.5	127.7	127.4
Θ(C1N2O4)	117.1	117.6	117.3
Θ(C1N2O3)	114.4	114.7	115.2
Θ(N2C1Cl5)	109.6	109.2	109.1
Θ(N2C1Cl6)	106.1	106.0	107.9
Φ(O4N2C1Cl5)	0.0	0.0	-22.0

The labeling of the atoms is as shown in Fig. 2. Bond lengths are in Å and angles in degrees

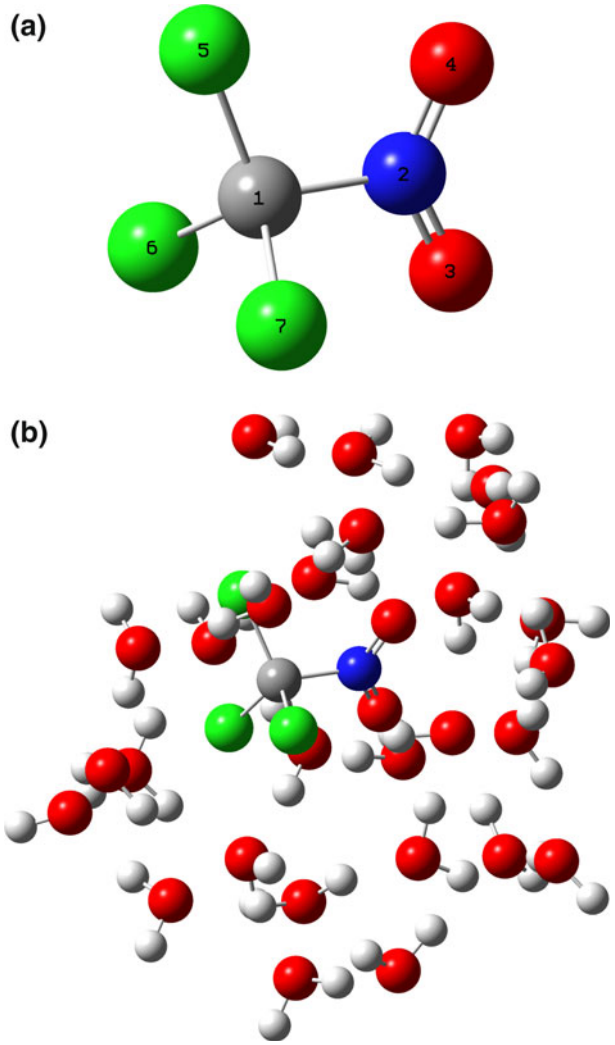

Fig. 2 **a** Chloropicrin molecule, showing the labeling of the atoms, **b** cluster of the chloropicrin solute, and 28 solvent water molecules. The point of view was selected, so that the atoms of chloropicrin are approximately in the same position as in **a**. Carbon is *gray*, nitrogen is *blue*, oxygens are *red*, chlorine atoms are *green*, and hydrogen atoms are *white*

The structure of chloropicrin in the simulated solvent or the cluster did not change much as compared to the gas phase, except in two aspects. The most noticeable difference, on one side, is that the stable conformer of chloropicrin in the cluster shows a relative rotation of 22° between the CCl_3 and NO_2 groups, while it was 0° both in gas phase and when the continuum was included. On the other side, inclusion of solvation increases the NO bond length, but while the continuum affects both bonds in the same way, the minimum structure in the cluster shows a more marked asymmetry between both NO bond lengths. It is also to be noticed that the specific interactions bring both CCl_3 and NO_2 groups closer, with a shorter CN distance,

Table 7 Frequencies (in cm^{-1}) and intensities (relative to the asymmetric stretching of the NO_2 group set at 100%) of the more interesting IR bands of chloropicrin in gas phase, within the continuum and in the cluster, calculated at the PBE0/6-31+G(d,p) level

Band	Gas phase		Continuum		Cluster	
	Frequency	Intensity	Frequency	Intensity	Frequency	Intensity
$\nu(CN)+\delta(CCl_3)$	732	12	722	15		
$\nu(CN)+\delta(NO_2)$	872	14	862	8	874	67
CNO_2 deform	882	44	867	44		
$\nu_{asym}(CCl_3)$	912	58	900	60	948	90
$\nu_{sym}(NO_2)$	1421	47	1432	36	1441	51
$\nu_{asym}(NO_2)$	1753	100	1744	100	1777	100

the opposite effect to that caused by the inclusion of the continuum simulation of the solvent.

The geometrical change in the cluster affects notoriously the symmetric and asymmetric NO_2 stretching bands. The $\nu_{sym}(NO_2)$ band was located at 1421 cm^{-1} with an intensity of 133 Km mol in gas phase and moved to 1440 cm^{-1} and a smaller intensity of 91 Km mol in the water cluster. This is a pure mode, involving none of the solvent water molecules. The $\nu_{asym}(NO_2)$ on the other side, which appeared at 1753 cm^{-1} (intensity 281) in gas phase, is not anymore a pure mode in the cluster but is heavily coupled to water motions. The two more intense vibrations where the asymmetric NO_2 vibration is participating occur at 1772 cm^{-1} (intensity 89 Km mol) and at 1777 cm^{-1} (intensity 178 Km mol). The more interesting IR bands are collected in Table 7, where the intensities are shown as relative to the asymmetric NO_2 vibration, arbitrarily set at 100. Some of the bands identified in gas phase are masked by the interaction of chloropicrin with the solvent, but the main effect is to decrease the intensity of the NO_2 stretching bands with respect to the CN stretching band. Full geometrical data, infrared transitions, and figures with the infrared spectra are included as supplementary material.

Acknowledgments This work was funded through project Comisión Sectorial de Investigación Científica (CSIC) 365/2006 (Universidad de la República, Uruguay). We also thank Programa de Desarrollo de las Ciencias Básicas (PEDECIBA) and Agencia Nacional de Investigación e Innovación (ANII) for partial financial support.

References

1. Öberg G (2002) Appl Microbiol Biotechnol 58:565–581
2. Keppler F, Borchers R, Pracht J, Rheinsberger S, Schöler HF (2002) Environ Sci Technol 36:2479–2483
3. Smidt H, de Vos WM (2004) Annu Rev Microbiol 58:43–73
4. Holliger C, Wohlfarth G, Diekert G (1999) FEMS Microbiol Rev 22:383–398
5. Pera-Titus M, García-Molina V, Baños MA, Giménez J, Esplugas S (2004) Appl Catal B Environ 47:219–256
6. Osborne RL, Raner GM, Hager LP, Dawson JH (2006) J Am Chem Soc 128:1036–1037
7. Fetzner S (1998) Appl Microbiol Biotechnol 50:633–657
8. Carter WPL, Luo D, Malkina IL (1997) Atmos Environ 31:1425–1439
9. Plewa MJ, Wagner ED, Jazwierska P, Richardson SD, Chen PH, McKague AB (2004) Environ Sci Technol 38:62–68
10. Castro CA, Wade RS, Belser NO (1983) J Agric Food Chem 31:1184–1187
11. Sparks SE, Quistad GB, Casida JE (1997) Chem Res Toxicol 10:1001–1007
12. Zheng W, Yates SR, Papiernik SK, Guo M (2006) J Agric Food Chem 54:2280–2287
13. Becke AD (1993) J Chem Phys 98:1372–1377
14. Perdew JP, Ernzerhof M, Burke K (1996) J Chem Phys 105:9982–9985
15. Curtiss LA, Raghavachari K, Pople JA (1993) J Chem Phys 98:1293–1298
16. Curtiss LA, Raghavachari K, Redfern PC, Rassolov V, Pople JA (1998) J Chem Phys 109:7764–7776
17. Curtiss LA, Redfern PC, Raghavachari K (2007) J Chem Phys 126:084108
18. Tomasi J, Mennucci B, Cammi R (2005) Chem Rev 105:2999–3093
19. Gaussian 03, Revision B.03, Frisch MJ, Trucks GW, Schlegel HB, Scuseria GE, Robb MA, Cheeseman JR, Montgomery JA Jr., Vreven T, Kudin KN, Burant JC, Millam JM, Iyengar SS, Tomasi J, Barone V, Mennucci B, Cossi M, Scalmani G, Rega N, Petersson GA, Nakatsuji H, Hada M, Ehara M, Toyota K, Fukuda R, Hasegawa J, Ishida M, Nakajima T, Honda Y, Kitao O, Nakai H, Klene M, Li X, Knox JE, Hratchian HP, Cross JB, Bakken V, Adamo C, Jaramillo J, Gomperts R, Stratmann RE, Yazyev O, Austin AJ, Cammi R, Pomelli C, Ochterski JW, Ayala PY, Morokuma K, Voth GA, Salvador P, Dannenberg JJ, Zakrzewski VG, Dapprich S, Daniels AD, Strain MC, Farkas O, Malick DK, Rabuck AD, Raghavachari K, Foresman JB, Ortiz JV, Cui Q, Baboul AG, Clifford S, Cioslowski J, Stefanov BB, Liu G, Liashenko A, Piskorz P, Komaromi I, Martin RL, Fox DJ, Keith T, Al-Laham MA, Peng CY, Nanayakkara A, Challacombe M, Gill PMW, Johnson B, Chen W, Wong MW, Gonzalez C, Pople JA (2004) Gaussian, Inc., Wallingford
20. Barss WM (1957) Chem Phys 27:1260–1266
21. Wade EA, Reak KE, Parsons BF, Clemes TP, Singmaster KA (2002) Chem Phys Lett 365:473–479
22. Haszeldine RN (1953) J Chem Soc 2525–2527
23. Agarwal UP, Barnes AJ, Orville-Thomas WJ (1985) Can J Chem 63:1705–1707
24. Ornellas FR (2000) Theor Chem Acc 103:469–476
25. Resende SM, Ornellas FR (2000) J Phys Chem A 104:11934–11939
26. Rayne S, Forest K (2010) Theochem 953:47–48
27. Jalkanen KJ, Degtyarenko IM, Nieminen RM, Cao X, Nafie LA, Zhu F, Barron LD (2008) Theor Chem Acc 119:191–210